

# We are IntechOpen, the world's leading publisher of Open Access books Built by scientists, for scientists

6,900

Open access books available

185,000

International authors and editors

200M

Downloads

Our authors are among the

154

Countries delivered to

TOP 1%

most cited scientists

12.2%

Contributors from top 500 universities



WEB OF SCIENCE™

Selection of our books indexed in the Book Citation Index  
in Web of Science™ Core Collection (BKCI)

Interested in publishing with us?  
Contact [book.department@intechopen.com](mailto:book.department@intechopen.com)

Numbers displayed above are based on latest data collected.  
For more information visit [www.intechopen.com](http://www.intechopen.com)



---

# Pseudo-gamma Spectrometry in Plastic Scintillators

---

Matthieu Hamel and Frédérick Carrel

Additional information is available at the end of the chapter

<http://dx.doi.org/10.5772/67134>

---

## Abstract

War against CBRN-E threats needs to continuously develop systems with improved detection efficiency and performances. This topic especially concerns the NR controls for homeland security. This chapter introduces how it is now possible to perform gamma identification using plastic scintillators, which are not conventionally designed for this purpose. Two distinct approaches are discussed: the first one is the chemical modifications of the scintillator itself and the second is introducing new algorithms, Specifically designed for this application.

**Keywords:** plastic scintillator, gamma spectrometry, metal loading, unfolding, homeland security

---

## 1. Introduction

Protection of civilians and facilities against chemical, biological, radiological, nuclear, and explosives (CBRN-E) emerged after 9/11 events and remains since this date of particular importance for countries and states. When combined to the shortage of efficient detectors (e.g.,  $^3\text{He}$  for thermal neutron detection) and a global, worldwide crisis, there is a real need of cheap, yet efficient detectors.

To detect illicit smuggling of gamma-ray sources, a first analysis requires fast gamma spectrometry. The abovementioned equation (increase in terrorists attack + need of cheap detectors for large-scale deployment) naturally leads one to use plastic scintillators (PS) as detectors to be embedded in radiation portal monitors. Despite its high gamma-ray sensitivity, this material is not perfectly suited for this, due mainly to the poor gamma resolution, Precluding therefore any subsequent gamma identification. In the case of gamma-rays emitters indeed, only the Compton continuum and Compton edge are obtained after interaction in the plastic scintillator, and no information of the full energy peak can be observed.

---

This chapter presents recent improvements concerning potential optimizations for the gamma-ray spectrometry using plastic scintillators as a detector, with a focus on:

- Chemically modifying the nature of the PS. Due to its intrinsic low density and effective atomic number, this family of detectors is not well-suited for gamma-ray spectrometry. However, recent advances in the loading of plastic scintillators with organometallic complexes containing, for example, lead, tin, or bismuth, led to important breakthroughs in this field. As a perspective, nanomaterials are now being included in plastic scintillators, which can afford new and unrevealed specifications. All the advantages and drawbacks of the plastic scintillator loading with organometallics will be fully discussed.
- Spectra classification and deconvolution methods based on specific smart algorithms have shown very promising results to identify gamma isotopes either alone or in mixtures. An important aspect for counterterrorism applications is real-time detection so algorithms which fulfill this requirement are of great interest.

This chapter mostly describes recent advances in the chemical modification of plastic scintillators for Pseudo-gamma spectrometry. The second part introduces dedicated algorithms for the processing of poorly resolved gamma-ray spectra, allowing therefore gamma identification with plastic scintillators [1]. When available, some examples will be provided.

## 2. Plastic scintillator modifications

### 2.1. Introduction to plastic scintillators

In a few words, a plastic scintillator is a fluorescent polymer which has the capability to emit photons when excited by an ionizing particle. The discovery and use was reported for the first time by Schorr and Torney as early as 1950 [1], as an extension of previous work on liquid scintillators.

The chemical formulation of a PS is usually composed of an aromatic matrix embedding one or several fluorophores. According to the Förster theory [2] (**Figure 1**), after radiation/matter interaction within the polymer, excitons are transferred from the matrix to the first fluorophore, then to the second fluorophore—so-called the wavelength shifter, allowing the incident energy response to emit close to 420 nm, for two reasons. This wavelength indeed corresponds to the maximum of quantum efficiency of traditional photomultiplier tubes (PMT's) and to the optical transparency domain of the material.

A typical composition of a plastic scintillator is the following (**Figure 2**):

- Matrix, generally based on polystyrene or polyvinyltoluene.
- Primary fluorophore, *p*-terphenyl or 2,5-diphenyloxazole (PPO) are global leaders, but many choices are possible.
- Secondary fluorophore, for example, 1,4-bis(5-phenyl-2-oxazolyl)benzene (POPOP), bis-methylstyrylbenzene (bis-MSB), 9,10-diphenylanthracene (9,10-DPA), etc.

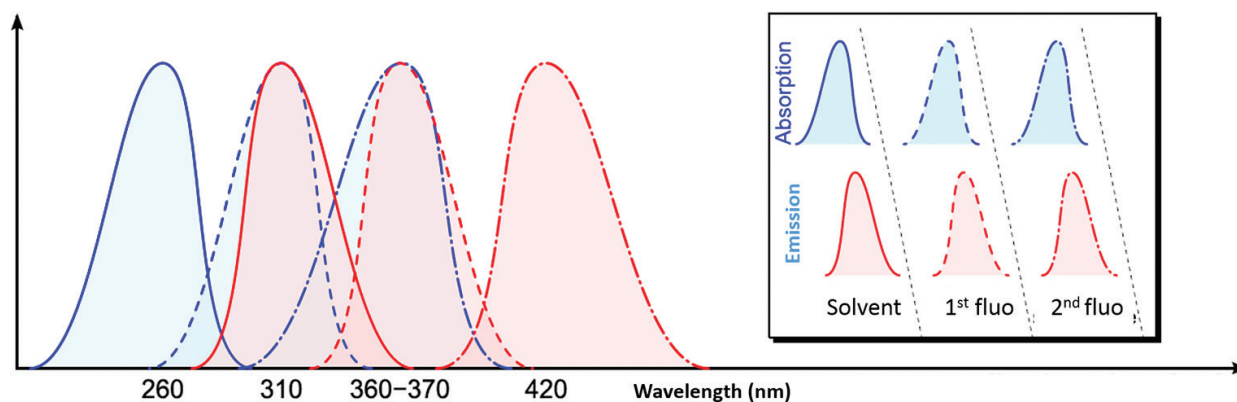


Figure 1. Schematic representation of the Förster theory typically used in liquid or plastic scintillators.

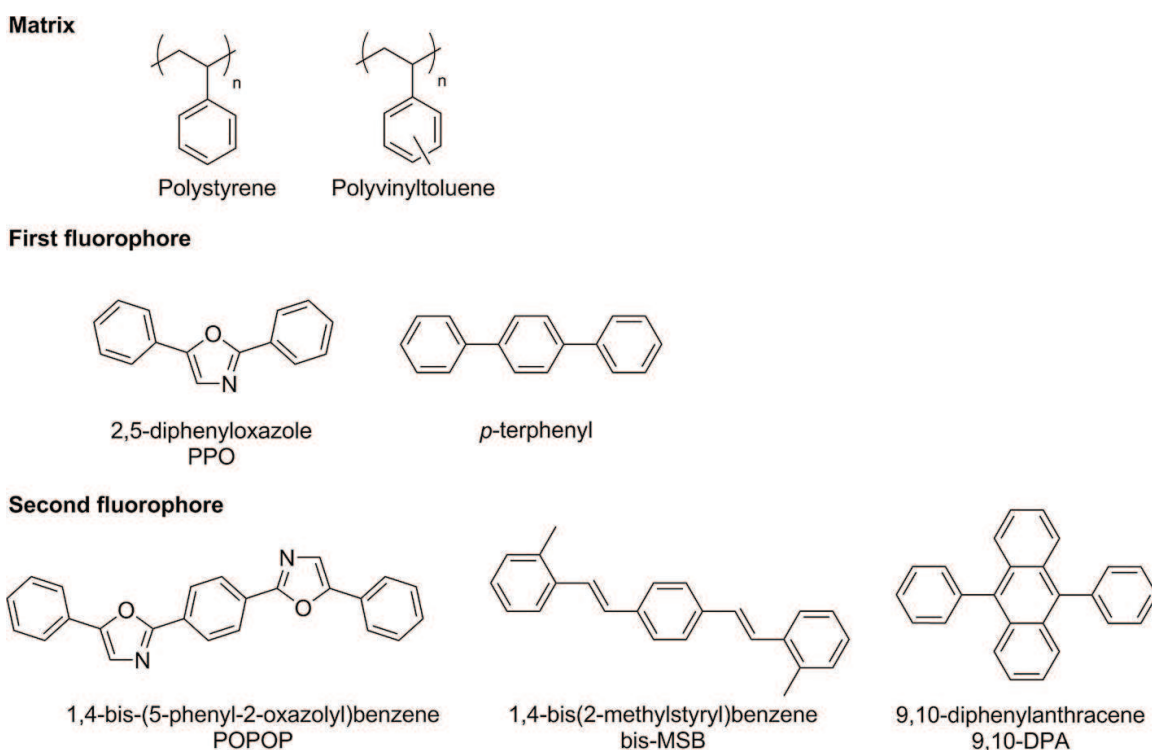


Figure 2. Schematic representations of molecules involved in the preparation of a plastic scintillator.

## 2.2. Plastic scintillator loading

According to this recipe, one can expect obtaining a regular plastic scintillator, with basic properties. Among other, it is noteworthy at this stage to introduce the scintillation light yield (or light output), which is the quantity of photons delivered by the material when excited by electrons with 1 MeV energy. When a special care is given to afford the plastic scintillator special applications—and this will be the topic of this chapter, it is possible to add various elements, for example, neutron absorbers or organometallics, the latter allowing the Pseudo-gamma spectrometry in plastic scintillators [3].

However, we will see that such loading may affect the light yield, leading to a trade-off between high metal content and detector's performances. In other words, a high loading may increase the effective atomic number ( $Z_{\text{eff}}$ ) of the material, but at the expense of its light output. Also of interest, not only the incident gamma-ray will be fully absorbed, but also the total count rate will benefit from the increase in the  $Z_{\text{eff}}$ .

### 2.3. Theory

It is known for a long time that only three main interaction mechanisms can occur at the same time in radiation measurement: Compton scattering, pair production, and the most important for gamma identification is the photoelectric effect.

To identify an incident radionuclide emitting gamma-rays, photoelectric absorption has to be favored. A rough approximation of the photoelectric effect probability is given by  $P_{pe} \approx \text{constant} \times Z_{\text{eff}}^n / (E_\gamma^{3.5})$ , where the exponent  $n$  varies between 4 and 5. This equation reveals the main drawback associated with plastic scintillators, namely their low effective atomic number. Calculating  $Z_{\text{eff}}$  for a PSt + 1.5 wt% *p*-terphenyl + 0.03 wt% POPOP scintillator composition gives a 5.7 value (PSt standing for polystyrene), which is too low to afford a sustainable photoelectric absorption. Thus, Compton scattering will be predominant, and full energy peaks can appear at 100, 300, and 500 keV for compounds with  $Z_{\text{eff}} \approx 15, 50$ , and 70, respectively [4].

To increase both density and  $Z_{\text{eff}}$ , chemists have turned their attention in loading plastic scintillators with heavy elements, affecting as low as possible the scintillation properties of the detector. This can be illustrated in **Figure 3** where one can see the appearance of the full energy peak on the black signal. To this, four strategies to host a metal inside a polymer matrix are possible. The first strategy to be explained is the most documented and uses organometallics, and the second most used involves nanoparticles. Two other strategies exist, namely dissolution of inorganic compounds and quantum dots, but so far they were not successfully applied to gamma-ray spectrometry; they are therefore not described in this chapter.

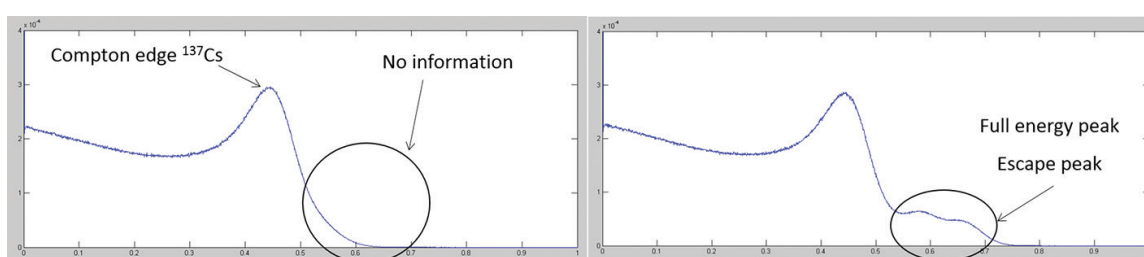


**Figure 3.** On the left:  $^{137}\text{Cs}$  spectrum using a standard plastic scintillator. On the right:  $^{137}\text{Cs}$  spectrum using a plastic scintillator doped with 5% lead. MCNPX simulation results. Same behavior expected for bismuth loading.

### 2.4. Heavy metal loading

#### 2.4.1. Organometallic complex

As already mentioned, the first plastic scintillator ever published was reported in 1950 [1]. Loading such materials with heavy metals took only three years to appear in a publication

[5]. This paved the way on the main characteristics the heavy metal loading has to fulfill: the organometallic complex must be highly soluble in the monomer, it must be stable, and a trade-off must be found between the gain obtained with the loading (herein the increase in the  $Z_{\text{eff}}$ ) and the metal quenching which will affect the light yield.

Basically, an organometallic complex is a molecule embedding a metal core surrounded by one or several organic ligands, their number depending on the valence of the metal. Lead-loaded plastic scintillators are already known and commercially available from several suppliers (**Table 1**). It is shown that the light output dramatically decreases when the metal concentration increases, due (logically) to metal quenching effect. Although not anymore commercially available, a tin-loaded plastic scintillator with metal concentration up to 7 wt% was sold by Nuclear Enterprise under the trade name NE140 [6].

Provider	Reference	[Pb] (wt%)	$\lambda_{\text{em}}$ (nm)	Light yield (ph/MeV) <sup>[c]</sup>	Light output/anthracene (%) <sup>[c]</sup>	Decay time (ns)
Saint-Gobain	BC-452	2, 5 or 10	424	4900	32	2.1
Eljen Technology	EJ-256	1 → 5 <sup>[a]</sup>	425	5200	34	2.1
Amcrys-H	n.d.	12 <sup>[b]</sup>	n.d.	n.d.	n.d.	n.d.
Rexon	RP-452	5	n.d.	5200	34	n.d.

n.d. denotes to not determined.

<sup>[a]</sup>Eljen Technology can raise the [Pb] up to 10 wt%, but these concentrations *are not recommended* [42].

<sup>[b]</sup>Also available as tin loading, up to 10 wt%.

<sup>[c]</sup>Spectroscopic data for 5 wt% loading.

**Table 1.** Commercial, lead-loaded plastic scintillators.

The choice of both metal and ligand(s) is of particular importance as it will directly affect the scintillation properties of the plastic scintillator. In the literature, the following metals were tested, with more or less popularity, at least in plastic solutions. Thus, Iodine [7] ( $Z = 53$ ), Holmium [8] ( $Z = 67$ ), Tantalum [8] ( $Z = 73$ ), and Mercury [9] ( $Z = 80$ ) were less studied. An extensive methodological work was performed by Sandler and Tsou concerning the metals from the groups IVA and VA [10]. An important statement was the fact that group VA metals are better quenchers than others of the group IVA.

Diphenylmercury(II) was used in the range 1–10 wt% of metal to load PS. The compound is of particular interest thanks to its high content (56.5%) of metal. Again a strong quenching effect was observed, with a 4-fold decrease in the light output from 1 to 10 wt%. Moreover, diphenylmercury failed to be sensitive to UV light.

Before being radioactive, the two heaviest metals reported in the Mendeleev table are lead and bismuth. Logically, they are also the most studied, along with tin. Thus, after Pichat [5], Hyman [11], Baroni [12], Dannin et al. [13–15] successfully observed for the first time a distinct photopeak emanating from the full energy absorption of the 662 keV,  $^{137}\text{Cs}$  gamma-ray. Herein, it is shown that full energy peaks are absent in lead-loaded plastic scintillators and

visible in 20–50 wt% of organometallic-loaded materials. Scintillators were composed of 3 wt% 2-(4-biphenyl)-5-phenyl-1,3,4-oxadiazole (PBD), 0.05 wt% POPOP, and either (4-ethylphenyl)-triphenyltin or *p*-triphenylstyryltin. The best observed photopeak resolution was 13%, obtained with a 30 wt% *p*-triphenylstyryltin (giving 7.86% of metal).

After almost 40 years of inactivity, new developments (mainly driven by the homeland security needs) have recently emerged, for all three recognized metals. Tin has been recently renewed with rationally designed complexes. Despite the lower *Z* of tin compared to lead or bismuth, the intersystem crossing—and by consequence the metal quenching effect—seems reduced for this metal [16]. An in-depth investigation has been performed in the synthesis of Tin(IV) organometallics in which the steric hindrance pushes back the fluorophore at distances in the range 5–20 Å. These compounds are typically alkyl- or aryl-derivatives of tin, either commercially available or prepared from the Grignard reaction of the organomagnesium halide with tin chloride. A plasticizing effect was observed when loading the material with tetra-(3-phenylpropyl)tin, which led to link the organometallic compound to the matrix *via* a methacrylate moiety. To afford the scintillation properties, 2-(4-*tert*-butylphenyl)-5-(4-biphenyl)-1,3,4-oxadiazole (butyl-PBD) was used as the dye. Thus, a 6% tin concentration was found as a trade-off between loading ratio and scintillation light yield, providing therefore the presence of photopeaks in the range 14 keV ( $^{241}\text{Am}$ ) to 1274 keV ( $^{22}\text{Na}$ ), with an 11.4% energy resolution at 662 keV. Ultimately, a cost projection was performed with such modified materials. It reveals that a 6 wt% tin-loaded PS could be roughly obtained at a 270 \$/kg (chemicals only).

Thanks to its low cost and high *Z*, lead is still of great interest. As lead(II) organometallics are very polar compounds, most strategies involve the use of polar comonomers to reach high concentrations. Significant improvements were also obtained when adding a polymerizable bond to the organic moiety of the organometallic complex. Thus, lead dimethacrylate ( $\text{Pb}(\text{MAA})_2$ ) is a candidate of choice for the 10–40 keV full X-ray absorption in plastic scintillators, allowing a metal loading as high as 27.4 wt% [17]. To allow parasite Cherenkov light effect rejection, this loading was coupled to high wavelength-shifting dyes, leading to 580 nm centered plastic scintillators. Unfortunately, the light yield was rather low (<1000 ph/MeV for 10.9 wt% of lead).

Very recently, a combined fast neutron/gamma discriminating lead-loaded plastic scintillator was reported [18]. This combines an organo-lead compound with PPO at a probable high concentration, this strategy being already known in the field of neutron detection [19]. The resolution is 16% at 662 keV, with a claimed scintillation yield of 9000 ph/MeV.

The last decade has seen many investigations on the synthesis of various bismuth organometallics and their application in plastic scintillator loading. Thanks to the very high solubility of triphenylbismuth in regular monomers such as styrene or vinyltoluene, one can expect elevated bismuth concentrations in the material. To overcome the metal quenching effect, Cherepy et al. proposed an exotic scintillator formulation based on a polyvinylcarbazole (PVK) matrix and a phosphorescent iridium complex. For samples as small as 1 cm<sup>3</sup>, the  $^{137}\text{Cs}$  pulse height spectrum exhibited several features isolated from bold deconvolutions, such as the full energy peak with a claimed resolution lower than 7%, along with the escape peak due to the  $^{209}\text{Bi}$  K $\alpha$  X-rays [20]. Bigger volume (48 cm<sup>3</sup>) allowed the full absorption of the 1274 keV gamma-ray from  $^{22}\text{Na}$  with a 9% resolution [21]. Later on, the PVK matrix was abandoned,

presumably due to the difficulty to scale up the material, and triphenylbismuth was substituted by bismuth tripivalate (**Figure 4**) [22]. Loadings of 29 wt% bismuth metal were reached without degraded transparency. A 6 wt% Bi-loaded sample showed a photopeak of  $^{137}\text{Cs}$  with a 15% resolution and a light yield close to 3300 ph/MeV.

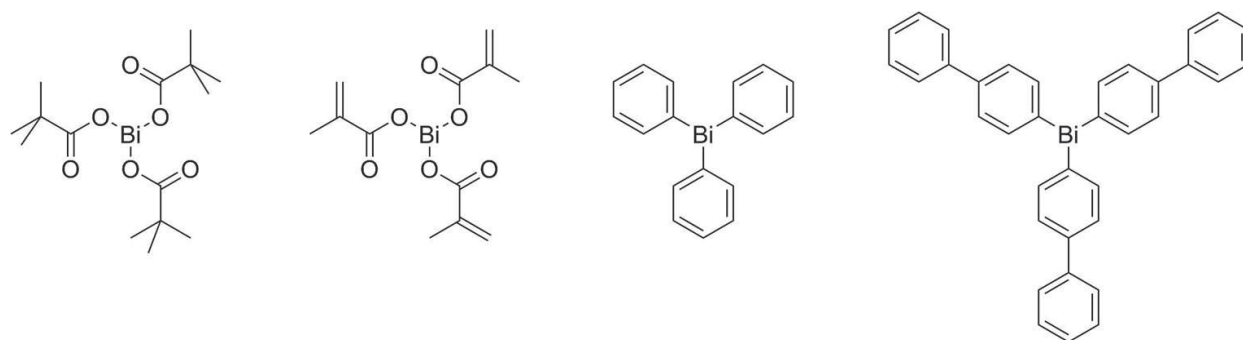


**Figure 4.** Examples of organo-bismuthine compounds used to load plastic scintillators: bismuth tripivalate, bismuth trimethacrylate, triphenylbismuth, and tris-biphenylbismuth (from left to right).

At the same time, Bertrand et al. designed both alkyl- and aryl-derivatives of bismuth(III) [23]. Bismuth tricarboxylates were easily prepared from the reaction between the carboxylic acid and  $\text{BiPh}_3$ , whereas tris-biphenylbismuth was isolated from the reaction between biphenyl lithium bromide with bismuth(III) chloride. A 6 wt% Bi-loaded sample revealed highly defined full energy peak for  $^{57}\text{Co}$  with a 122 keV energy and a light yield close to 4600 ph/MeV. Interestingly, a linear increase in both photoelectric and Compton count rates obtained from the corresponding integration of the region was observed from 0 to 9 wt% of bismuth; the dataset at 11 wt% reveals however a decrease, showing here that the high amount of metal becomes noxious and does not give clear compensation to the loss of scintillation yield. Later on, a 155 cm<sup>3</sup> sized sample containing 5 wt% of bismuth was reported by the same group. A good trend was observed for the full absorption of 67.4 keV X-rays [24]; however, no full energy peak was observed when the scintillator was irradiated with  $^{137}\text{Cs}$  gamma source [25].

#### 2.4.2. Nanomaterials

Loading PS with nanomaterials emerge as a new field, and not only for gamma-ray spectrometry, as can be proven for instance with lithium loading for thermal neutron capture [26]. The differences between an organometallic complex and a nanomaterial arise in the sense that the metal core is constituted from a metal salt surrounded by an organic shell, and the global size of the molecule is at the nanometer scale, giving therefore unrevealed feature.

As an application to the gamma-ray spectrometry field, the first example was reported by Cai et al. [27, 28] The composite scintillator was composed of a polyvinyltoluene (PVT) matrix embedding gadolinium oxide ( $\text{Gd}_2\text{O}_3$ ) nanocrystals as the gamma sensitizer, along with a rather unusual fluorophore for scintillation purpose, namely 4,7-bis-{2'-9',9'-bis[(2''-ethylhexyl)-fluorenyl]}-2,1,3-benzothiadiazole (FBtF). FBtF shows an appreciable Stokes shift

with a dual excitation maxima at 310 and 420 nm (most probably the  $S_0 \rightarrow S_2$  and  $S_0 \rightarrow S_1$  transitions, respectively), and an emission maximum around 520 nm. To allow the dispersion of  $Gd_2O_3$  in the composite, it was capped with both oleic acid and oleylamine (**Figure 5**).

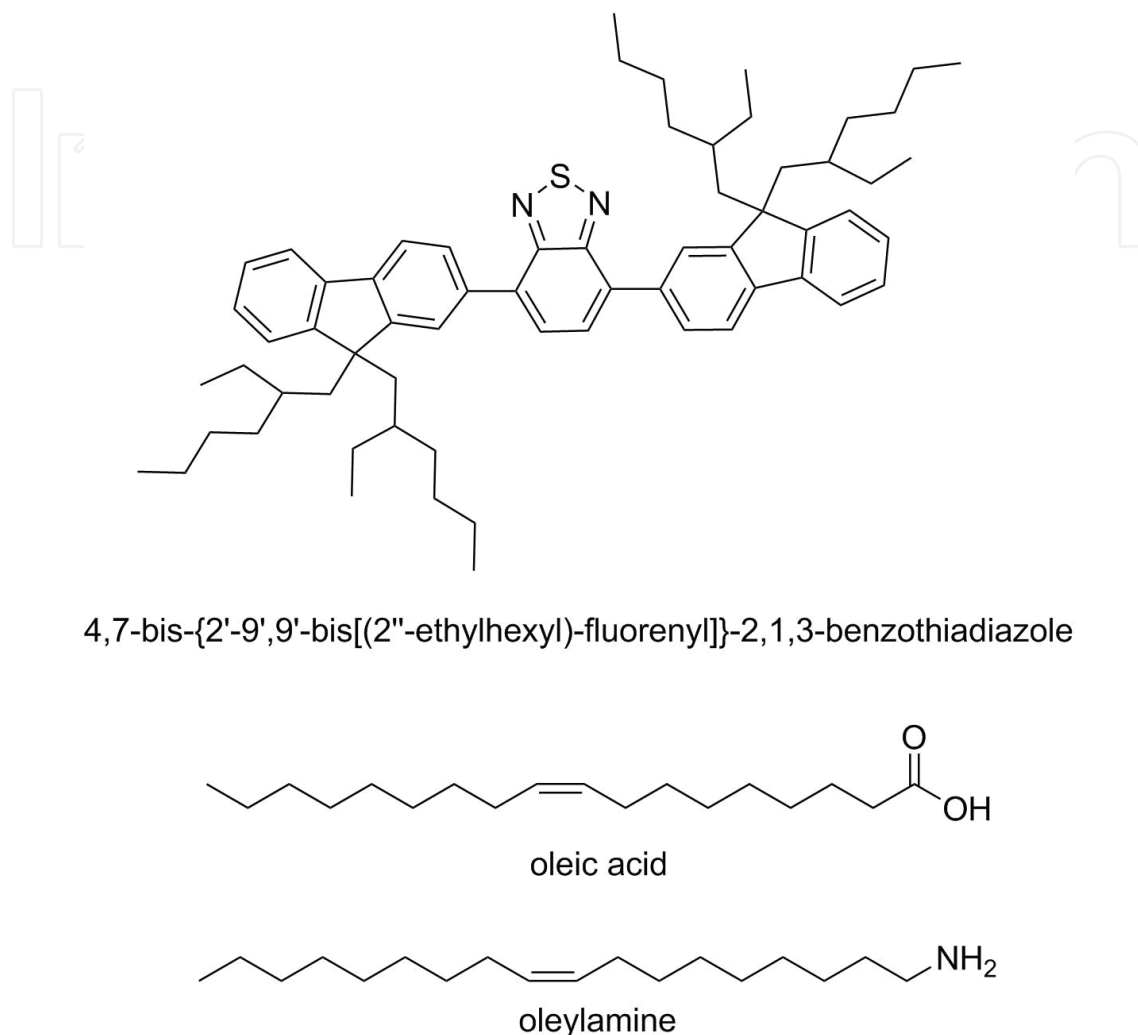


**Figure 5.** Topological representation of FBtF (top), oleic acid (middle), and oleylamine (bottom).

Thus, small and transparent monoliths ( $\Phi$  14 mm, thickness 3 mm) were successfully obtained with a Gd loading as high as 31 wt%. While excited with 662 keV gamma-rays, a full energy peak with an 11.4% energy resolution was observed.

The same group extended this work to hafnium oxide nanoparticles composite scintillators [29]. The nanocomposite monolith of 1 cm diameter and 2 mm thickness shows a full energy photopeak for 662 keV gamma-rays, with the best unfolded full energy peak resolution <8%. Ultimately, ytterbium fluoride nanoparticles with loading as high as 63 wt% were prepared [30]. Composites loaded with 20 wt% of  $YbF_3$  show the full energy peak of  $^{137}Cs$  with an estimated 8600 ph/MeV light yield.

Hafnium-doped organic-inorganic hybrid scintillators were fabricated *via* a sol-gel method [31]. This consists in  $Hf_xSi_{1-x}O_2$  obtained from the sol-gel reaction of hafnium oxychloride

with phenyltrimethoxysilane dissolved in PSt, with a maximum Hf loading of 10 wt%. Other examples were reported with zirconium oxide nanoparticles loaded in PSt for 67.4 keV X-rays [32]. Loadings up to 30 wt% have been achieved. Significantly higher X-ray excited luminescence was also observed with barium fluoride nanoparticles [33]. Again high loadings (40 wt%) are possible, albeit at the expense of the optical transmission.

### 3. Algorithms

#### 3.1. Context and motivations

Identification of radionuclides emitting gamma-rays is one of the main challenging topics related to nuclear measurements. This issue is crucial in several fields of nuclear industry. For instance, this step is of great interest in the frame of decommissioning applications or for obtaining a performing storage of nuclear waste packages. Nowadays, identification of radionuclides is considered as a crucial issue for homeland security applications. This important step is for instance required for identifying radioactive material potentially hidden with naturally occurring radioactive materials (NORM).

Gamma-ray spectrometry is the reference line of attack for identifying radionuclides and has been used for decades by scientific and industrial communities. Using appropriate detectors, this technique enables to obtain both qualitative (nature of radionuclides) and quantitative (activity of a given radionuclide) information. However, in the frame of homeland security applications, high detection efficiency is often required and the use of large size detectors became a crucial topic, so plastic scintillators are of great interest. However, due to their intrinsic characteristics, these detectors are not adapted to gamma-ray spectrometry measurements using standard methods.

For several years, alternative methods were developed by different research teams in order to overcome limitations related to detectors having a poor energy resolution. General principle followed by these teams is based on a global analysis of the gamma-ray spectrum and not only on restricted areas of interest in the latter, usually corresponding to a full energy deposition.

#### 3.2. Standard approach for gamma-ray spectrometry analysis and associated limitations

Gamma-ray spectrometry is a technique based on the detection of Gamma-rays emitted by specific radionuclides. This method enables to qualitatively identify radionuclides as well as to quantify their activity. The information of interest is extracted from the full energy peak, which corresponds to a full energy deposition of the incident Gamma-ray. For instance,  $^{137}\text{Cs}$  has a characteristic gamma-ray emission at 661.7 keV and the presence of  $^{60}\text{Co}$  is associated with the emission of two Gamma-rays at 1173.2 and 1332.5 keV. Using reference database (for instance, ENDF, JEFF, LARA databases [34], etc.), it is possible to identify the radionuclide from a raw gamma spectrum (a calibration step of the detector using well-known sources is required). Concerning the activity information, the latter could be obtained by extracting the net peak area from selected regions in the spectrum. The net peak area corresponds to the gross number of counts in the region of interest minus the background continuum underlying beneath the peak and due to Compton interactions. The ability of discriminating peaks

close in energy and extracting their net peak areas are two of the most important features for gamma-ray spectrometry applications.

Detectors used for gamma-ray spectrometry measurements can be segmented into two categories: scintillators and semiconductors. As previously mentioned, the quality of a detector for gamma-ray spectrometry measurements can be evaluated considering two main parameters: its energy resolution (ability to discriminate two peaks in a spectrum close in energy) and its absolute efficiency (number of counts detected in the full energy peak region per emitted Gamma-ray). Both these parameters can significantly change according to the type of the detector. Inorganic scintillators (sodium iodide NaI(Tl), bismuth germanate BGO) have a degraded resolution in comparison with those related to semiconductors (cadmium zinc telluride CZT or high purity germanium HPGe). As an illustration, the standard energy resolution of a NaI(Tl) detector is equal to 7.5% at 661.7 keV, compared to 1 keV for HPGe detector. However, inorganic scintillators often have better detection efficiency. Indeed, due to their low cost, it is possible to produce them in larger dimensions. Some recent technological development, like LaBr<sub>3</sub> scintillators, can be considered as a good trade-off for spectrometry measurements (standard energy resolution equal to 3% at 661.7 keV). **Figure 6** compares <sup>152</sup>Eu spectra, respectively, obtained using a HPGe detector and a NaI(Tl) scintillator. For the latter, full energy peaks can be distinguished, but the extraction of net peak areas is more complicated than for the analysis of HPGe spectra.

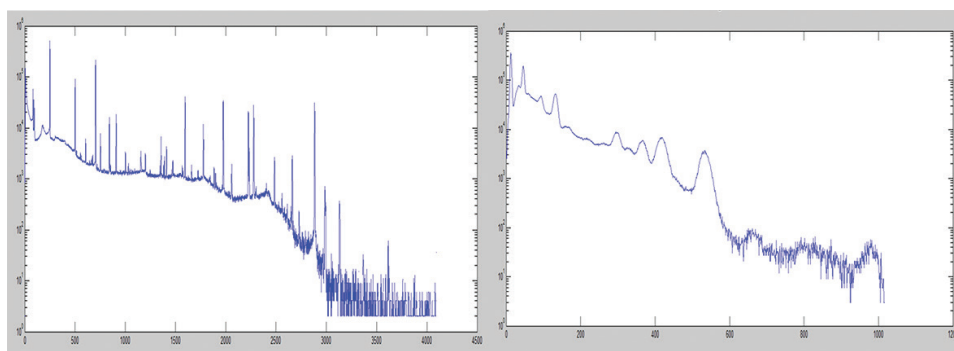


**Figure 6.** Example of <sup>152</sup>Eu experimental spectra using a HPGe semiconductor (on the left) or a NaI(Tl) scintillator (on the right).

On the other side, plastic scintillators are a category of detectors generally devoted to counting applications. For several years, they have been extensively used for homeland security applications. Indeed, productions costs are extremely low, and these detectors can be manufactured in very large dimensions (for instance, an EJ-200 plastic scintillator with dimensions 10 cm × 10 cm × 100 cm, costs 2000 euros per unit). For this reason, there is a lot of interest for extending capacities offered by these detectors, especially adding spectrometric functionalities. However, due to their intrinsic characteristics (plastic scintillators are mainly composed by carbon and hydrogen, corresponding to a  $Z_{\text{eff}}$  of 5.7 and a density of 1.02) and despite very large dimensions in comparison with other detectors, the probability to have a full energy deposition is very low in the active volume. **Figure 7** illustrates a simulated spectrum

of a plastic scintillator in the presence of  $^{137}\text{Cs}$  and  $^{60}\text{Co}$  sources. The reference Monte Carlo MCNPX code is used to carry out this simulation step [35]. Full energy peaks cannot be identified in the spectrum, but only Compton edges which are often used for energy calibration. For this reason, alternative methods are required to qualitatively and quantitatively process such degraded spectra.

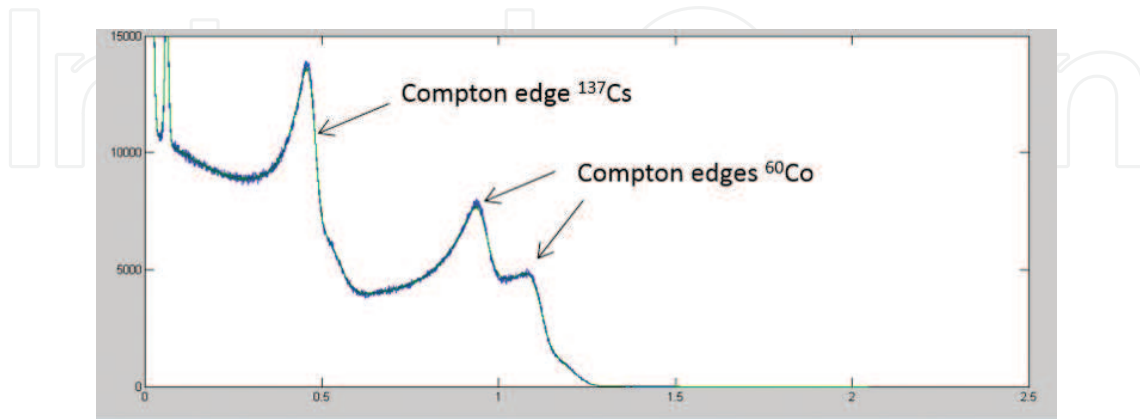


**Figure 7.** Example of a gamma-ray spectrum obtained with a plastic scintillator (EJ-200 type),  $^{137}\text{Cs}$  and  $^{60}\text{Co}$  signatures (Monte Carlo simulation using MCNPX).

As it was mentioned in the first part of this chapter, intensive work has been carried out by several research teams for several years in order to enhance the spectrometric performances of plastic scintillators. **Figure 8** illustrates the difference between gamma-ray spectra obtained with a standard plastic scintillator and a 5 wt% lead-loaded plastic scintillator (simulation result using MCNPX). Interesting features due to lead loading are present in the last case (small full energy peak and escape peak). However, a specific spectrum processing is still required to carry out a performing identification step.

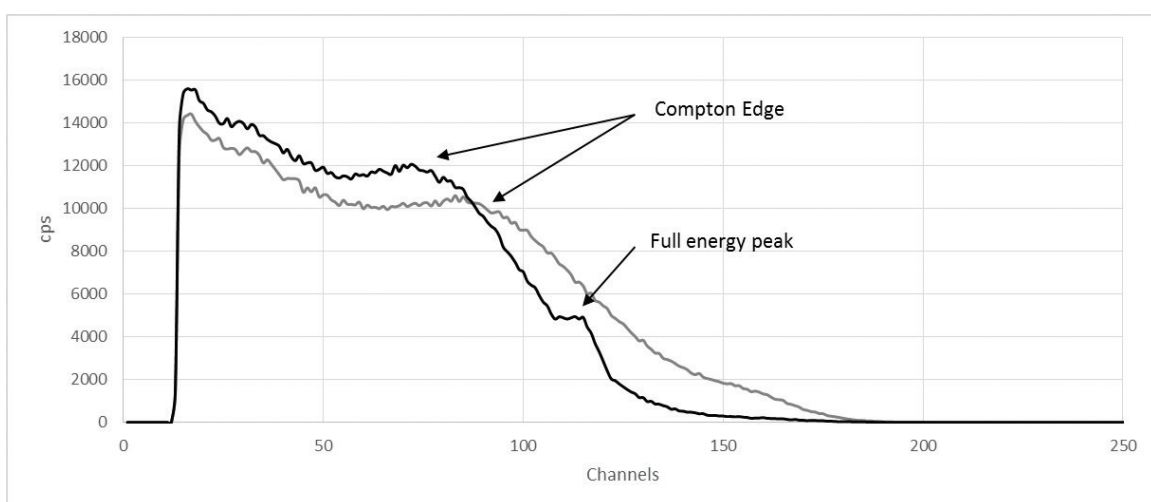


**Figure 8.** Example of a  $^{137}\text{Cs}$  gamma pulse height spectra with a standard (gray line) and a metal-loaded PS allowing the visualization of a full energy peak.

### 3.3. Analysis of a gamma-ray spectrum as an inverse problem

A potential alternative for analyzing gamma-ray spectra having a poor energy resolution consists of processing the complete spectrum and not only slight regions of interest focused on full energy peaks. In this way, the processing of a gamma-ray spectrum appears as an inverse problem (classical approach for instance for tomographic applications) and can be solved using a specific reconstruction algorithm. Following this methodology, the analysis of a gamma-ray spectrum can be considered under the following matrix form:

$$S = H \cdot A \quad (1)$$

where:

- $S$  is called the signal matrix: matrix of dimensions ( $nbe\_channels, 1$ ). The  $nbe\_channels$  parameter corresponds to the number of channels of the gamma-ray spectrum. The  $S$  matrix corresponds to the measurement result, that is, the gamma-ray spectrum to be processed.
- $A$  is called the activity matrix: matrix of dimensions ( $nbe\_incident\_energies, 1$ ). The  $nbe\_incident\_energies$  parameter corresponds to the number of incident energies defined by the user and considered during the reconstruction process. These incident energies correspond to the number of voxels (elemental volumes) of a standard emission tomography problem. The  $A$  matrix corresponds to the result of the reconstruction.
- $H$  is called the transfer matrix of the problem: matrix of dimensions ( $nbe\_channels, nbe\_incident\_energies$ ). This matrix integrates all detection efficiencies taken into account in the inverse problem. For instance, the element  $h_{ij}$  corresponds to the probability that a photon of incident energy equal to  $j$  was detected in the channel  $i$  of the gamma-ray spectrum. Roughly speaking, it can be seen as a reference database from which the deconvolution step will be carried out.

In this way, the  $H$  matrix contains the spectrometric behavior of a detection system for each incident energy defined by the user and considered in the problem. It is important to emphasize that the data processing will be further carried out on this incident energy grid. For this reason, the choice of the grid energy step is a crucial parameter to obtain a performing reconstruction.

Another manner to define the  $H$  matrix consists of directly considering gamma-ray signatures of specific radionuclides (for instance,  $^{241}\text{Am}$ ,  $^{137}\text{Cs}$ ,  $^{60}\text{Co}$ , etc.) and not individual incident gamma-ray energies. In this case, the  $H$  matrix has the dimensions ( $nbe\_channels, nbe\_radionuclides$ ) and the reconstruction step directly enables to obtain the proportion of a given radionuclide in the spectrum. The parameter  $nbe\_radionuclides$  corresponds to the number of radionuclides defined by the end user and considered in the problem.

The definition of the  $H$  matrix is one of the most important points of this technique. Two approaches are possible to determine this parameter. The use of Monte Carlo simulations is a first possibility. Several Monte Carlo codes like MCNPX, GEANT4, or TRIPOLI are indeed available and can be considered as performing solutions to determine the behavior of a detector for a given incident energy. The main benefit of this solution concerns its flexibility. Indeed, it is possible to simulate any incident energy or experimental configuration and to minimize in this way experimental constraints due to the calibration step. On the other side, the drawback of

this method is mainly related to the accuracy of the Monte Carlo model and its consistency with the experimental behavior of the real detector. A discrepancy between the simulated gamma-ray spectrum and the real behavior of the detector will have a direct impact on the result of the reconstruction. The importance of this impact will be fully related to the agreement between simulated and experimental results. For this reason, an accurate simulation is required for both the detector and its environment which is somehow tricky, especially for the low-energy part of the spectrum (energy range <200 keV, strong impact of Compton effects due to the environment).

The other solution consists of an experimental calibration of the detector itself using reference sources. The number of experimental radionuclides is also reduced in comparison with a Monte Carlo simulation-based methodology, and it will directly define the grid for the reconstruction step (only the database approach can be considered in this way). However, the great benefit of this solution is to obtain the exact experimental behavior of the detector for a given radionuclide, without bias in comparison with the simulation.

The reconstruction step is the second key parameter of this process. First of all, it is important to emphasize that a direct inversion of the formula given previously cannot be considered for solving such problems. Indeed,  $S$  or  $H$  matrices coefficients have intrinsic statistical uncertainties, and a direct inversion can lead to nonphysical values (for instance, negative activity values, which are of course non-consistent with a physical behavior). Development of specific algorithms has been a topic of interest for the research community for several decades, and many scientific articles were published on this subject. For instance, we can cite the linear regularization system (also named as the Phillips-Twomey approach [36]) or the method based on the maximum of entropy [37] (MEM). One of the most literature-cited methods is based on the approach called maximum likelihood-expectation maximization [38] (ML-EM). In comparison with Phillips-Twomey or MEM methods, ML-EM enables to take into account the Poisson nature of the experimental data given as an input of the problem. An example of applications of this type of algorithm for this current topic can be found in Ref. [39]. Finally, the ML-EM approach can be extended to the Bayesian MAP-EM (maximum a posteriori-expectation maximization) algorithm which introduces an a priori law on the incident energy grid.

Both ML-EM and MAP-EM are iterative techniques, and these algorithms converge to a solution enabling to maximize likelihood. An important point concerns the initial values taken at the beginning of the analysis. A standard procedure consists of considering that all the coefficients of the  $A$  matrix have the same values before the first iteration.

### 3.4. Analysis on simulated and experimental data

**Figure 9** illustrates results obtained for the deconvolution of gamma-ray spectra following an inverse problem methodology. A cocktail of radioactive sources is simulated using the Monte Carlo MCNPX code ( $^{241}\text{Am}$ ,  $^{137}\text{Cs}$ ,  $^{60}\text{Co}$ ) for a standard plastic scintillator. An ML-EM algorithm is used for processing the gamma-ray spectrum. As previously mentioned, we can see that only Compton edges can be identified in the input gamma-ray spectrum. On the right, it is possible to see the result obtained after the deconvolution process in terms of incident energies. The main peaks given as input parameters of the simulation can be clearly identified (59.5 keV for  $^{241}\text{Am}$ , 661.7 keV for  $^{137}\text{Cs}$ , 1173.2 and 1332.5 keV for  $^{60}\text{Co}$ ). Moreover, as the  $H$  matrix integrates the efficiency of interest, the result after deconvolution direct gives

an activity value (same intensity for instance for both peaks of  $^{60}\text{Co}$  after deconvolution). However, it is important to mention that the incident energy obtained after the analysis corresponds to a value allowed by the grid of incident energies (for instance, considering the peak due to  $^{137}\text{Cs}$ , the rebuilt incident energy is spread between 660 and 670 keV, due to the binning defined by the end user). **Figure 10** illustrates processing on the same simulated data but considering this time the database approach (deconvolution on a family of radionuclides and not on incident energies). It should be noted that results presented in **Figure 10** have been obtained using a different algorithm than ML-EM (nonparametric Bayesian methodology).

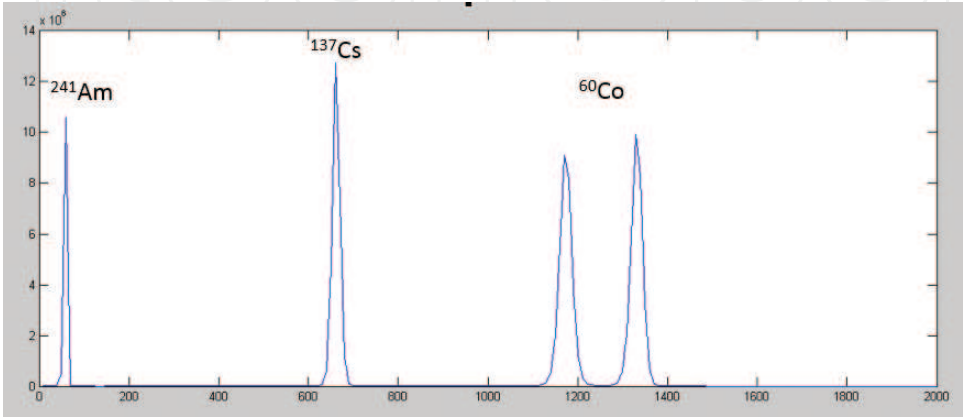


**Figure 9.** Incident energies of a gamma sources mixtures ( $^{241}\text{Am}$ ,  $^{137}\text{Cs}$ , and  $^{60}\text{Co}$ ) obtained after processing with an inverse problem approach [41].

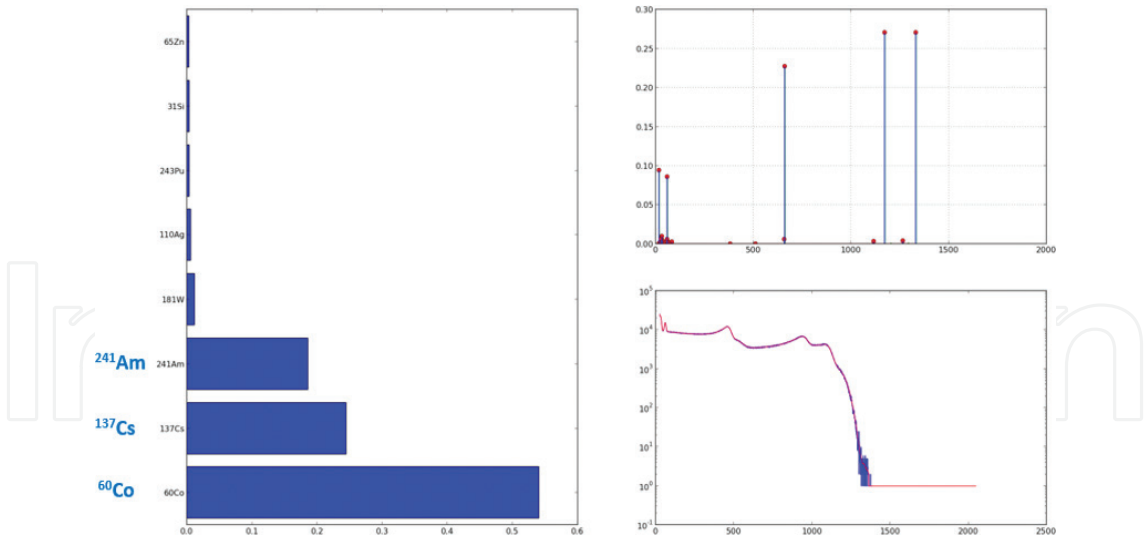


**Figure 10.** On the left: nature and associated proportion of radionuclides present in the gamma-ray spectrum. On the right: Gamma-rays associated with the detected radionuclides and comparison between simulated (blue curve) and rebuilt gamma-ray spectra (red curve).

### 3.5. Current status and future developments

**Table 2** summarizes breakthroughs obtained in the field of metal loading.

Metal additive (wt%)	Organometallic compound	Matrix	Full energy peak absorption (keV)	Resolution (%)	$\gamma$ light yield <sup>[a]</sup> (ph/MeV)	Typical sample size (cm <sup>3</sup> )	Ref.
Sn (7.8)	<i>p</i> -triphenylstyryltin	PVT	662	13	≈6000	n.g.	[10]
Sn (6)	Tributyltinmethacrylate	PSt	662	11.4	6700	6.4	[17]
Pb (n.g.)	n.g.	PSt	662	16	9000	n.g.	[19]
Bi (19.0)	Triphenylbismuth	PVK	662	6.8	7200	1	[21]
Bi (21.3)	Triphenylbismuth	PVK	1275	9	≈12,000	48	[22]
Bi (6)	Bismuth tripivalate	PVT	662	15	3300	103	[23]
Bi (5)	Triphenylbismuth	PSt	122	78	3900	155	[26]
Bi (8)	Acetyldimethacrylylbismuth	PSt	122	n.g.	2500	20.8	[24]
Gd (3.1) <sup>[b]</sup>	Gd <sub>2</sub> O <sub>3</sub> nanocrystals	PVT	662	11.4	n.g. <sup>[c]</sup>	0.46	[28]
Yb (15)	YbF <sub>3</sub> nanoparticles	PVT	662	n.g.	8600	0.16	[31]
Hf (28.5)	HfO <sub>2</sub>	PVT	662	8	≈10,000	0.16	[30]
Hf (10)	Hf <sub>x</sub> Si <sub>1-x</sub> O <sub>2</sub>	PSt	67.4 <sup>[d]</sup>	n.g.	4560	<1	[32]
Zr (22)	ZrO <sub>2</sub> nanoparticles	PSt	67.4 <sup>[d]</sup>	n.g.	n.g.	<1	[33]

n.g. denotes to not given.  
<sup>[a]</sup>When not explicitly given, evaluated from the gamma spectrum.  
<sup>[b]</sup>Based on a calculated volume density.  
<sup>[c]</sup>A beta light yield is given with <sup>204</sup>Tl excitation, showing 27,000 ph/MeV, relative to BC-400 plastic scintillator.  
<sup>[d]</sup>X-rays excitation.

**Table 2.** Main improvements leading to gamma-ray spectrometry with plastic scintillators.

Gamma-ray counting or spectrometry enhancement with plastic scintillator loading is a pretty old strategy, but new key technologies allow now identifying gamma-ray spectra with various energies. This is extremely mandatory for the future generation radiation portal monitors used in homeland security. Most of the design is now performed with organometallic compounds mainly with tin, lead, and bismuth organometallics, but we have seen herein that other solutions may be of great value. Loading inorganics in plastic scintillators is obviously the cheapest method, but this method will be rapidly limited in terms of metal concentration and optical transparency. Metal-encapsulated nanoparticles would represent the most affordable and efficient in terms of gamma-ray spectrometry, but the described samples usually stand at the cm<sup>3</sup> state, so not big enough to find an application in radiation portal monitors.

Analysis of gamma-ray spectra using innovative methods is of great interest for identifying radionuclides, especially for homeland security applications where there is a real need for this type of features. Analysis methods based on a global processing of the gamma-ray spectrum are a performing way to identify radionuclides as soon as detectors with poor energy resolution are used. Several challenges can be identified as mid-term and long-term perspectives for developing and improving such algorithms. First of all, for homeland security applications, a second-order analysis is often required (for instance, if a moving object like a truck should be analyzed) and the processing time should be reduced as low as possible. Several teams developed identification solutions well adapted to address this challenge (see for instance Ref. [40]). Another issue strongly impacting this family of methods concerns the accuracy of the database used during the deconvolution step and its consistency with the gamma-ray spectrum to be measured. If the radioisotope is hidden by a specific shielding, the measured gamma-ray spectrum will be modified accordingly, and a bias will be introduced in comparison with the reference signature, potentially impacting the reconstruction step. Finally, coupling the algorithmic part with modified plastic scintillators, including for instance Bi loading, could improve the identification step because of the apparition of specific features in the spectrum, like full energy and escape peaks.

## Author details

Matthieu Hamel\* and Frédérick Carrel\*

\*Address all correspondence to: matthieu.hamel@cea.fr; frederick.carrel@cea.fr

CEA, LIST, Laboratoire Capteurs and Architectures Électroniques, CEA Saclay, Gif-sur-Yvette, France

## References

- [1] Schorr MG, Torney FL. Solid non-crystalline scintillation phosphors. *Physical Reviews* 1950;**80**:474. doi:10.1103/PhysRev.80.474
- [2] Förster T. Zwischenmolekulare Energiewanderung und Fluoreszenz. *Annalen der Physik* 1948;**437**(1–2):55–75. doi:10.1002/andp.19484370105

- [3] Bertrand GHV, Hamel M, Sguerra F. Current status on plastic scintillators modifications. *Chemistry – A European Journal* 2014;**20**(48):15660–15685. doi:10.1002/chem.201404093
- [4] Evans RD. *The Atomic Nucleus*. McGraw-Hill Company; 1955. p. 712. doi:10.1002/aic.690020327
- [5] Pichat L, Pesteil P, Clément J. Solides fluorescents non cristallins pour mesure de radio-activité. *Journal de Chimie Physique et de Physico-Chimie Biologique* 1953;**50**:26–41.
- [6] Cho ZH, Tsai CM, Eriksson LA. Tin and lead loaded plastic scintillators for low energy gamma-ray detection with particular application to high rate detection. *IEEE Transactions on Nuclear Science* 1975;**NS-22**(1):72–80. doi:10.1109/TNS.1975.4327618
- [7] Zhao YS, Yu Z, Douraghy A, Chatziioannou AF, Mo Y, Pei Q. A facile route to bulk high-Z polymer composites for Gamma-ray scintillation. *Chemical Communications* 2008:6008–6010. doi:10.1039/b813571a
- [8] Britvich GI, Vasil'chenko VG, Lapshin VG, Solov'ev AS. New heavy plastic scintillators. *Instruments and Experimental Techniques* 2000;**43**(1):36–39. doi:10.1007/BF02758995
- [9] Basile LJ. Characteristics of plastic scintillators. *The Journal of Chemical Physics* 1957;**27**:801–806. doi:10.1063/1.1743832
- [10] Sandler SR, Tsou KC. Quenching of the scintillation process in plastics by organometallics. *The Journal of Physical Chemistry* 1964;**68**:300–304. doi:10.1021/j100784a015
- [11] Hyman Jr. M, Ryan JJ. Heavy elements in plastic scintillators. *IRE Transactions on Nuclear Science*. 1958;**5**(3):87–90. doi:10.1109/TNS2.1958.4315631
- [12] Baroni EE, Kilin SF, Lebsadze TN, Rozman IM, Shoniya VM. Addition of hetero-organic compounds to polystyrene. *Soviet Atomic Energy* 1964;**17**(6):1261–1264. doi:10.1007/BF01122774
- [13] Sandler SR, Tsou KC. Evaluation of organometallics in plastic scintillators towards gamma-radiation. *The International Journal of Applied Radiation and Isotopes* 1964;**15**(7):419–426. doi:10.1016/0020-708X(64)90140-1
- [14] Dannin J, Sandler SR, Baum B. The use of organometallic compounds in plastic scintillators for the detection and resolution of Gamma-rays. *The International Journal of Applied Radiation and Isotopes* 1965;**16**(10):589–597. doi:10.1016/0020-708X(65)90095-5
- [15] Sandler SR, Dannin J, Tsou KC. Copolymerization of *p*-Triphenyltinystyrene and *p*-Triphenylleadstyrene with Styrene or Vinyltoluene. *Journal of Polymer Science | Part A, Polymer Chemistry* 1965;**3**:3199–3207. doi:10.1002/pol.1965.100030914
- [16] Feng PL, Mengesha W, Anstey MR, Cordaro JG. Distance dependent quenching and gamma-ray spectroscopy in tin-loaded polystyrene scintillators. *IEEE Transactions on Nuclear Science* 2016;**63**(1):407–415. doi:10.1109/TNS.2015.2510960
- [17] Hamel M, Turk G, Rousseau A, Darbon S, Reverdin C, Normand S. Preparation and characterization of highly lead-loaded red plastic scintillators under low energy

- X-rays. *Nuclear Instruments and Methods in Physics Research Section A: Accelerators, Spectrometers, Detectors and Associated Equipment* 2011;**660**(1):57–63. doi:10.1016/j.nima.2011.08.062
- [18] van Loef E, Markosyan G, Shirwadkar U, McClish M, Shah K. Gamma-ray spectroscopy and pulse shape discrimination with a plastic scintillator. *Nuclear Instruments and Methods in Physics Research Section A: Accelerators, Spectrometers, Detectors and Associated Equipment* 2015;**788**:71–72. doi:10.1016/j.nima.2015.03.077
- [19] Bertrand GHV, Hamel M, Normand S, Sguerra F. Pulse shape discrimination between (fast or thermal) neutrons and Gamma-rays with plastic scintillators: State of the art. *Nuclear Instruments and Methods in Physics Research Section A: Accelerators, Spectrometers, Detectors and Associated Equipment* 2015;**776**:114–128. doi:10.1016/j.nima.2014.12.024
- [20] Rupert BL, Cherepy NJ, Sturm BW, Sanner RD, Payne SA. Bismuth-loaded plastic scintillators for gamma-ray spectroscopy. *Europhysics Letters* 2012;**97**:22002. doi:10.1209/0295-5075/97/22002
- [21] Cherepy NJ, Sanner RD, Tillotson TM, Payne SA, Beck PR, Hunter S, Ahle L, Thelin PA. Bismuth-loaded plastic scintillators for gamma spectroscopy and neutron active interrogation. *IEEE Nuclear Science Symposium and Medical Imaging Conference Record (NSS/MIC)* 2012:1972–1973. doi:10.1109/NSSMIC.2012.6551455
- [22] Cherepy NJ, Sanner RD, Beck PR, Swanberg EL, Tillotson TM, Payne SA, Hurlbut CR. Bismuth- and lithium-loaded plastic scintillators for gamma and neutron detection. *Nuclear Instruments and Methods in Physics Research Section A: Accelerators, Spectrometers, Detectors and Associated Equipment* 2015;**778**:126–132. doi:10.1016/j.nima.2015.01.008
- [23] Bertrand GHV, Sguerra F, Dehé-Pittance C, Carrel F, Coulon R, Normand S, Barat É, Dautremer T, Montagu T, Hamel M. Influence of bismuth loading in polystyrene-based plastic scintillators for low energy gamma spectroscopy. *Journal of Materials Chemistry C* 2014;**2**:7304–7312. doi:10.1039/c4tc00815d
- [24] Koshimizu M, Bertrand GHV, Hamel M, Kishimoto S, Haruki R, Nishikido F, Yanagida T, Fujimoto Y, Asai K. X-ray Detection Capabilities of bismuth-doped Plastic Scintillators. *Japanese Journal of Applied Physics* 2015;**54**:102202. doi:10.7567/JJAP.54.102202
- [25] Bertrand GHV, Dumazert J, Sguerra F, Coulon R, Corre G, Hamel M. Understanding behavior of different metals in loaded scintillators: discrepancy between gadolinium and bismuth. *Journal of Materials Chemistry C* 2015;**3**:6006–6011. doi:10.1039/c5tc00387c
- [26] Carturan SM, Marchi T, Maggioni G, Gramegna F, Degerlier M, Cinausero M, Palma MD, Quaranta A. Thermal neutron detection by entrapping  $^6\text{LiF}$  nanocrystals in siloxane scintillators. *Journal of Physics: Conference Series* 2015;**620**:012010. doi:10.1088/1742-6596/620/1/012010

- [27] Cai W, Chen Q, Cherepy N, Dooraghi A, Kishpaugh D, Chatziioannou A, Payne S, Xiang W, Pei Q. Synthesis of bulk-size transparent gadolinium oxide–polymer nanocomposites for Gamma-ray spectroscopy. *Journal of Materials Chemistry C* 2013;**1**:1970–1976. doi:10.1039/c2tc00245k
- [28] Chen Q, Cai W, Hajagos T, Kishpaugh D, Liu C, Cherepy N, Dooraghi A, Chatziioannou A, Payne S, Pei Q. Bulk-Size Transparent Gadolinium Oxide-Polymer Nanocomposites for Gamma-ray Scintillation. *Nanotechnology 2014: Graphene, CNTs, Particles, Films & Composites, Technical Proceedings of the NSTI Nanotechnology Conference and Expo 2014*:1:295–296. ISBN: 978-1-4822-5826-4
- [29] Liu C, Hajagos TJ, Kishpaugh D, Jin Y, Hu W, Chen Q, Pei Q. Facile single-precursor synthesis and surface modification of hafnium oxide nanoparticles for nanocomposite  $\gamma$ -ray scintillators. *Advanced Functional Materials* 2015;**25**(29):4607–4616. doi:10.1002/adfm.201501439
- [30] Jin Y, Kishpaugh D, Liu C, Hajagos TJ, Chen Q, Li L, Chen Y, Pei Q. Partial ligand exchange as a critical approach to synthesizing transparent ytterbium fluoride-polymer nanocomposite monoliths for Gamma-ray scintillation. *Journal of Materials Chemistry C* 2016;**4**:3654–3660. doi:10.1039/C6TC00447D
- [31] Sun Y, Koshimizu M, Yahaba N, Nishikido F, Kishimoto S, Haruki R, Asai K. High-energy X-ray detection by hafnium-doped organic-inorganic hybrid scintillators prepared by sol-gel method. *Applied Physics Letters* 2014;**104**:174104. doi:10.1063/1.4875025
- [32] Araya Y, Koshimizu M, Haruki R, Nishikido F, Kishimoto S, Asai K. Enhanced detection efficiency of plastic scintillators upon incorporation of zirconia nanoparticles. *Sensors and Materials* 2015;**27**(3):255–261. doi:10.18494/SAM.2015.1063
- [33] Demkiv TM, Halyatkin OO, Vistovskyy VV, Gektin AV, Voloshinovskii AS. Luminescent and kinetic properties of the polystyrene composites based on BaF<sub>2</sub> nanoparticles. *Nuclear Instruments and Methods in Physics Research Section A: Accelerators, Spectrometers, Detectors and Associated Equipment* 2016;**810**:1–5. doi:10.1016/j.nima.2015.11.130
- [34] Java-based nuclear information software (JANIS). Available from: <http://www.nea.fr/janis> [accessed 2016-07-26].
- [35] Briesmeister JF. MCNP<sup>TM</sup> – A General Monte Carlo N-Particle Transport Code – Version 4C, Los Alamos National Laboratory report LA-13709-M, 2000.
- [36] Phillips DL. A technique for the numerical solution of certain integral equations of the first kind. *Journal of the ACM* 1962;**9**(1):84–97. doi:10.1145/321105.321114
- [37] Jaynes ET. How does the brain do plausible reasoning? In Erickson GJ, Smith CR, editors. *Maximum-Entropy and Bayesian Methods in Science and Engineering*. Foundations. Kluwer Academic Publishers; 1988. Vol 1. pp. 1–24. doi:10.1007/978-94-009-3049-0\_1
- [38] Shepp LA, Vardi Y. Maximum likelihood reconstruction for emission tomography. *IEEE Transactions on Medical Imaging* 1982;**1**(2):113–122. doi:10.1109/TMI.1982.4307558

- [39] Burt C. Plastic Scintillation Spectrometry. PhD dissertation. Southampton University; 2009. Available from: <http://eprints.soton.ac.uk/72351/1.hasCoversheetVersion/Thesis.pdf> [last accessed 2017-01-05].
- [40] Corre G, Boudergui K, Sannié G, Kondrasovs V. A Generic Isotope Identification Approach for nuclear instrumentation, In: IEEE proceedings of Advancements in Nuclear Instrumentation Measurement Methods and their Applications; 20–24 April 2015; Lisbon. IEEE; 2016. doi:10.1109/ANIMMA.2015.7465628
- [41] Hamel M, Dehé-Pittance C, Coulon R, Carrel F, Pillot P, Barat É, Dautremer T, Montagu T, Normand S. Gammastic: towards a pseudo-gamma spectrometry in plastic scintillators. In: IEEE proceedings of Advancements in Nuclear Instrumentation Measurement Methods and their Applications; 23–27 June 2013; Marseille. IEEE; 2014. doi:10.1109/ANIMMA.2013.6727889
- [42] EJ-256 data sheet. Available from: <http://www.eljentechnology.com/index.php/products/plastic-scintillators/ej-256> [last accessed 2016-07-26].